

Zooming in on ‘bi-large’ neutrino mixing with the first JUNO results

Gui-Jun Ding,^{1,*} Ranjeet Kumar,^{2,†} Newton Nath,^{3,‡} Rahul Srivastava,^{2,§} and José W. F. Valle^{4,¶}

¹*Department of Modern Physics, and Anhui Center for fundamental sciences in theoretical physics,
University of Science and Technology of China, Hefei, Anhui 230026, China*

²*Department of Physics, Indian Institute of Science Education and Research - Bhopal
Bhopal Bypass Road, Bhauri, Bhopal, India*

³*Department of Physics, Indian Institute of Technology (BHU), Varanasi 221005, India*

⁴*AHEP Group, Institut de Física Corpuscular – CSIC/Universitat de València, Parc Científic de Paterna.
C/ Catedrático José Beltrán, 2 E-46980 Paterna (Valencia) - SPAIN*

The leptonic mixing matrix is examined within bi-large mixing patterns and confronted with the latest results announced by the Jiangmen Underground Neutrino Observatory (JUNO). We analyze the viability of bi-large mixing schemes and assess JUNO’s ability to test neutrino mixing and discriminate among different bi-large mixing patterns, some of which are strongly disfavored when compared with neutrino oscillation global-fit results. Specific octant and CP predictions emerge. Finally, we comment on the implications of JUNO’s findings for neutrinoless double beta decay.

I. INTRODUCTION

The next-generation Jiangmen Underground Neutrino Observatory (JUNO) has released its first measurements of two of the neutrino oscillation parameters, Δm_{21}^2 and $\sin^2 \theta_{12}$, based on 59.1 days of data. The reported best-fit values with 1σ uncertainties are [1]

$$\sin^2 \theta_{12} = 0.3092 \pm 0.0087, \quad \Delta m_{21}^2 = (7.50 \pm 0.12) \times 10^{-5} \text{ eV}^2, \quad (1)$$

for the normal neutrino mass ordering scenario. Recently, the SNO+ collaboration also reported new measurements of reactor antineutrino oscillations [2]. When combined with the PDG 2025 global dataset [3], the updated best-fit oscillation parameters are $\sin^2 \theta_{12} = 0.310 \pm 0.012$, $\Delta m_{21}^2 = (7.63 \pm 0.17) \times 10^{-5} \text{ eV}^2$.

Remarkably, the JUNO results already surpass the precision of current neutrino oscillation global-fit determinations [4–8]. This improved precision provides an important new input for testing theoretical frameworks of lepton mixing and significantly sharpens constraints on many flavour

* Email Address: [dinggg@ustc.edu.cn](mailto:dingga@ustc.edu.cn)

† Email Address: ranjeet20@iiserb.ac.in

‡ Email Address: mnath.phy@iitbhu.ac.in

§ Email Address: rahul@iiserb.ac.in

¶ Email Address: valle@ific.uv.es

models [9–15]. At the current juncture, the unknowns in the neutrino oscillation sector include the neutrino mass ordering (i.e., the sign of Δm_{31}^2 , with $\Delta m_{31}^2 > 0$ referred to as normal ordering and $\Delta m_{31}^2 < 0$ as inverted ordering), the octant of the atmospheric mixing angle θ_{23} (i.e., $\theta_{23} < 45^\circ$ for the lower octant and $\theta_{23} > 45^\circ$ for the upper octant), and the CP-violating phase δ . Considerable theoretical and experimental efforts are currently underway to predict and determine these unknowns. With the release of first data from JUNO, there have already been several attempts to assess the impact of these precision measurements of oscillation parameters on existing theoretical frameworks [16–24]. However, it becomes more challenging to develop theoretical models that describe the increasingly precise experimental data. Indeed, there have been several recent theoretical approaches to understand neutrino mixing and oscillations [9–15].

Motivated by the latest precision measurements from JUNO, we examine the framework of bi-large neutrino mixing, as proposed in [25–27], which provides sharp predictions for the neutrino mixing parameters. The idea behind such mixing patterns relies on the observation that the smallest lepton mixing angle is numerically close to the largest quark mixing angle. This leads to the hypothesis that the Cabibbo angle may serve as a universal seed for both quark and lepton mixings. Such bi-large mixing paradigm have already inspired some approaches for describing the structure of the lepton mixing matrix [25–27]. Recently, more refined variants of this approach have been proposed [28, 29], further motivating an updated analysis in light of the improved experimental precision reached in JUNO.

The lepton mixing matrix is the leptonic analogue of the Cabibbo-Kobayashi-Maskawa (CKM) matrix. It is defined as

$$U = U_\ell^\dagger U_\nu, \quad (2)$$

where U_ℓ and U_ν denote the diagonalization matrices associated with the charged-lepton and neutrino sectors, respectively. The peculiar pattern of its matrix elements has intrigued theorists ever since neutrino oscillations were discovered. This interest has only intensified following reactor measurements confirming that $\theta_{13} \neq 0$ [30, 31] and T2K results suggesting a nearly maximal value of the leptonic CP-violating phase δ [32]. Several attempts have been made to account for the non-zero value of θ_{13} [33–37], including deviations from the conventional tribimaximal mixing pattern [38, 39], which can yield realistic descriptions of neutrino oscillation data [40, 41].

In this work, we examine the compatibility of bi-large proposals for the leptonic mixing matrix by confronting them with the latest JUNO measurement as well as global analysis of neutrino oscillation data [4, 6, 7]. In addition to the bi-large *ansatz* for the neutrino diagonalization matrix U_ν , these schemes include a charged-lepton correction factor U_ℓ , taken to be “CKM-like,” as motivated by Grand Unified Theories (GUTs). Our approach follows the same general strategy as the symmetry-based sensitivity studies performed in the context of the DUNE experiment in Refs. [42–47]. Our present study is specifically tailored to address the impact of the recent JUNO data on the bi-large lepton mixing schemes. We determine the allowed regions of the oscillation parameters within each bi-large *ansatz* and discuss the prospects for distinguishing among the different bi-large scenarios.

II. BI-LARGE MIXING PATTERNS

Here we present an overview of the predictions of bi-large mixing patterns for the lepton mixing matrix. For concreteness, we focus on the patterns T1 and T2 from Ref. [28], while T3 and T4 are taken from the earlier work in Ref. [27]. Following Ref. [27], we assume that the bi-large patterns arise from simple Grand Unified Theory (GUT) constructions, in which the charged-lepton and down-type quark sectors exhibit similar structure.

Type-1 (T1)

The first bi-large pattern, **T1**, assumes that the neutrino mixing angles are correlated with the Cabibbo angle as follows [28]

$$\sin \theta_{23} = 1 - \lambda, \quad \sin \theta_{12} = 2\lambda, \quad \sin \theta_{13} = \lambda. \quad (3)$$

Truncating to $\mathcal{O}(\lambda^2)$, we obtain the neutrino factor of the mixing matrix U_{BL1} as

$$U_{BL1} \approx \begin{bmatrix} 1 - \frac{5\lambda^2}{2} & 2\lambda & -\lambda \\ \lambda - 2\sqrt{2}\lambda^{3/2} & \sqrt{2\lambda} - \frac{\lambda^{3/2}}{2\sqrt{2}} & 1 - \lambda - \frac{\lambda^2}{2} \\ 2\lambda + \sqrt{2}\lambda^{3/2} & -1 + \lambda & \sqrt{2\lambda} - \frac{\lambda^{3/2}}{2\sqrt{2}} \end{bmatrix}. \quad (4)$$

By itself U_{BL1} alone does not account for the full leptonic mixing matrix. To obtain a realistic mixing matrix consistent with current oscillation data, we must include the appropriate charged-lepton corrections to U_{BL1} . For this case, the $SO(10)$ GUT-motivated, CKM-like charged-lepton corrections are given by

$$U_{l_1} = R_{23}(\theta_{23}^{CKM}) \Phi R_{12}(\theta_{12}^{CKM}) \Phi^\dagger \approx \begin{bmatrix} 1 - \frac{1}{2}\lambda^2 & \lambda e^{-i\phi} & 0 \\ -\lambda e^{i\phi} & 1 - \frac{1}{2}\lambda^2 & A\lambda^2 \\ A\lambda^3 e^{i\phi} & -A\lambda^2 & 1 \end{bmatrix}. \quad (5)$$

Here we use $\sin \theta_{12}^{CKM} = \lambda$ and $\sin \theta_{23}^{CKM} = A\lambda^2$, where $\lambda = 0.22501 \pm 0.00068$ and $A = 0.826^{+0.016}_{-0.015}$ are the Wolfenstein parameters [3]. We also define $\Phi = \text{diag}\{e^{-i\phi/2}, e^{i\phi/2}, 1\}$, with ϕ treated as a free parameter. The lepton mixing matrix for **T1** is then given by $U = U_{l_1}^\dagger U_{BL1}$, from which the mixing angles and the leptonic Jarlskog invariant J_{CP} follow as

$$\begin{aligned} \sin^2 \theta_{13} &\approx 4\lambda^2(1 - \lambda) \cos^2 \frac{\phi}{2}, \\ \sin^2 \theta_{12} &\approx 2\lambda^2(2 - 2\sqrt{2\lambda} \cos \phi + \lambda), \\ \sin^2 \theta_{23} &\approx (1 - \lambda)^2 - 2\sqrt{2}A\lambda^{5/2} - 2\lambda^3(1 + 2 \cos \phi), \\ J_{CP} &\approx -2 \left(\sqrt{2} + \sqrt{\lambda} \right) \lambda^{5/2} \sin \phi. \end{aligned} \quad (6)$$

Note that, besides the leading order term, there is a $-2\lambda^3 \sin \phi$ contribution in J_{CP} .

Type-2 (T2)

In the second bi-large pattern, **T2**, we relate the neutrino mixing angles to the Cabibbo angle as follows [28],

$$\sin \theta_{23} = 3\lambda, \quad \sin \theta_{12} = 2\lambda, \quad \sin \theta_{13} = \lambda \quad (7)$$

and approximate the neutrino diagonalization matrix as

$$U_{BL2} \approx \begin{bmatrix} 1 - \frac{5\lambda^2}{2} & 2\lambda & -\lambda \\ -2\lambda + 3\lambda^2 & 1 - \frac{13\lambda^2}{2} & 3\lambda \\ \lambda + 6\lambda^2 & -3\lambda + 2\lambda^2 & 1 - 5\lambda^2 \end{bmatrix} \quad (8)$$

Motivated by $SU(5)$ unification, here we take the charged-lepton diagonalization matrix to be

$$U_{l_2} = \Phi^\dagger R_{12}^T(\theta_{12}^{CKM}) \Phi R_{23}^T(\theta_{23}^{CKM}) \approx \begin{bmatrix} 1 - \frac{1}{2}\lambda^2 & -\lambda e^{i\phi} & A\lambda^3 e^{i\phi} \\ \lambda e^{-i\phi} & 1 - \frac{1}{2}\lambda^2 & -A\lambda^2 \\ 0 & A\lambda^2 & 1 \end{bmatrix}, \quad (9)$$

where θ_{12}^{CKM} , θ_{23}^{CKM} , and Φ have the same definitions as given below Eq. (5). Using the forms of U_{BL2} and U_{l_2} , we construct the lepton mixing matrix for **T2** as $U = U_{l_2}^\dagger U_{BL2}$. The resulting mixing angles and the leptonic Jarlskog invariant J_{CP} are

$$\begin{aligned} \sin^2 \theta_{13} &\approx \lambda^2 - 6\lambda^3 \cos \phi + 8\lambda^4, \\ \sin^2 \theta_{12} &\approx \lambda^2(5 + 4 \cos \phi) - 2\lambda^4(8 + 13 \cos \phi), \\ \sin^2 \theta_{23} &\approx 9\lambda^2 + 6\lambda^3(A + \cos \phi) - \lambda^4(8 - 2A \cos \phi - A^2), \\ J_{CP} &\approx -[3 + (16 + A)\lambda] \lambda^3 \sin \phi, \end{aligned} \quad (10)$$

where the next-to-leading-order contribution $-(16 + A)\lambda^4 \sin \phi$ in J_{CP} is included, as it is comparable in size to the leading-order term.

Type-3 (T3)

The patterns **T3** and **T4** require, in addition to the standard Wolfenstein parameters λ and A , two other free parameters ψ and δ in order to fully characterize their physical lepton mixing matrices. To first order approximation, the three neutrino mixing angles are assumed to be of the following form,

$$\sin \theta_{12} = \sin \theta_{23} = \psi \lambda, \quad \sin \theta_{13} = \lambda. \quad (11)$$

where ψ is a free parameter whose value is determined by fitting to neutrino oscillation data. From Eq. (11) it follows that the neutrino diagonalization matrix U_{BL3} is given by

$$U_{BL3} = \begin{bmatrix} c\sqrt{1-\lambda^2} & \psi\lambda\sqrt{1-\lambda^2} & \lambda \\ -c\psi\lambda(1+\lambda) & c^2 - \psi^2\lambda^3 & \psi\lambda\sqrt{1-\lambda^2} \\ -c^2\lambda + \psi^2\lambda^2 & -c\psi\lambda(1+\lambda) & c\sqrt{1-\lambda^2} \end{bmatrix}, \quad c \equiv \cos \sin^{-1}(\psi\lambda). \quad (12)$$

For the case of **T3**, we take the charged-lepton diagonalization matrix to be the same as U_{l_1} in Eq. (5). With this choice, we can obtain the following expressions for the lepton mixing parameters:

$$\begin{aligned} \sin^2 \theta_{13} &\approx \lambda^2 - 2\psi\lambda^3 \cos \phi + (-1 + 2Ac \cos \phi + \psi^2) \lambda^4, \\ \sin^2 \theta_{12} &\approx (c^4 - 2c^2\psi \cos \phi + \psi^2) \lambda^2 + (c^4 - \psi^2) \lambda^4, \\ \sin^2 \theta_{23} &\approx \psi^2\lambda^2 + 2(\cos \phi - Ac) \psi\lambda^3 + (1 - \psi^2 - 2Ac \cos \phi + A^2c^2) \lambda^4, \\ J_{CP} &\approx c^2 [\psi + (\psi - Ac - \psi^3) \lambda] \lambda^3 \sin \phi. \end{aligned} \quad (13)$$

Type-4 (T4)

For this bi-large mixing pattern, **T4**, we again take the neutrino part of the mixing matrix to be identical with U_{BL3} , as given in Eq. (12). The distinction between the **T3** and **T4** patterns arises from the choice of charged-lepton corrections. In contrast to the **T3** pattern, which uses the matrix U_{l_1} , here we adopt the charged-lepton diagonalization matrix U_{l_2} introduced in Eq. (9). This modification leads to different predictions for the lepton mixing parameters. In this setup, the lepton mixing angles and the Jarlskog invariant are determined to be:

$$\begin{aligned} \sin^2 \theta_{13} &\approx \lambda^2 + 2\psi\lambda^3 \cos \phi - (1 - \psi^2) \lambda^4, \\ \sin^2 \theta_{12} &\approx (c^4 + 2c^2\psi \cos \phi + \psi^2) \lambda^2 + (c^4 - \psi^2) \lambda^4, \\ \sin^2 \theta_{23} &\approx \psi^2\lambda^2 + 2(Ac - \cos \phi) \psi\lambda^3 + (1 - \psi^2 - 2Ac \cos \phi + A^2c^2) \lambda^4, \\ J_{CP} &\approx c^2 [\psi + (\psi + Ac - \psi^3) \lambda] \lambda^3 \sin \phi. \end{aligned} \quad (14)$$

Having introduced the full set of bi-large mixing patterns including their corresponding charged-lepton corrections, we now proceed in the next section to examine their phenomenological implications in light of recent JUNO results and other current neutrino oscillation data

III. STATUS OF BI-LARGE MIXING BEFORE JUNO'S θ_{12} MEASUREMENT

The predictions of the four bi-large mixing patterns discussed here can be tested in number of neutrino oscillation experiments. Before exploring the impact of recent JUNO results, let us briefly investigate their status before the inclusion of JUNO data, updating the study given in [29]. The

status of the bi-large mixing patterns can be nicely encoded through the $(\sin^2 \theta_{23} - \delta)$, $(\sin^2 \theta_{13} - \delta)$, and $(\sin^2 \theta_{13} - \sin^2 \theta_{23})$ oscillation parameter correlation plots.

We examined the status of bi-large mixing schemes taking into account the global-fit of the world's oscillation data sample presented in [4]. Our results are given in Fig. 1. Among all four patterns, **T1** remains the most compatible with the oscillation data, successfully describing the best-fit values in the $(\sin^2 \theta_{23} - \delta)$ plane as well as $(\sin^2 \theta_{13} - \sin^2 \theta_{23})$ plane. The **T2** pattern is consistent at the 2σ confidence level in the $(\sin^2 \theta_{23} - \delta)$ plane, at the lower octant region. In contrast, **T3** is excluded by the current global-fit at the 3σ confidence level (see the magenta curve), while **T4** falls barely inside it. With improved precision in the measurement of δ , the **T4** pattern is expected to be ruled out in the near future.

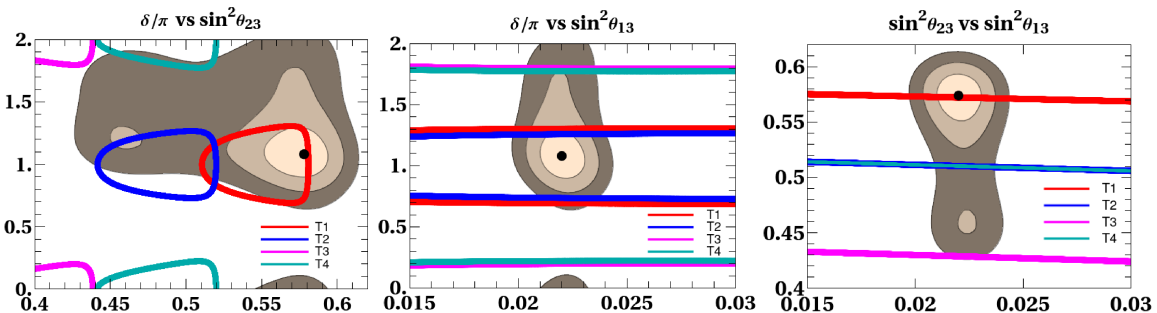


FIG. 1. Status of bi-large mixing pattern given the global oscillation fit in [4, 5]. The red, blue, magenta, and cyan branches correspond to the **T1**, **T2**, **T3**, and **T4** patterns, respectively.

IV. STATUS OF BI-LARGE MIXING PATTERNS AFTER JUNO'S PRECISION MEASUREMENT

The Jiangmen Underground Neutrino Observatory (JUNO) is a multipurpose, large-volume liquid-scintillator neutrino experiment designed primarily to determine the neutrino mass ordering with high statistical significance. The detector is located at a baseline of about 53 km from the Yangjiang and Taishan nuclear power plants, optimized to resolve oscillation effects associated with both the solar and atmospheric mass-squared differences [4, 6, 7]. JUNO consists of a 20 kton central detector filled with linear alkylbenzene liquid scintillator, viewed by approximately 18,000 high-quantum-efficiency 20-inch PMTs together with an additional system of about 25,000 3-inch PMTs, yielding an unprecedented energy resolution of roughly $3\%/\sqrt{E(\text{MeV})}$ [1]. The experiment aims to achieve sub-percent precision on the solar mixing parameters θ_{12} , Δm_{21}^2 , and $|\Delta m_{31}^2|$, as well as to measure the reactor antineutrino spectrum with high accuracy, with the potential to probe new physics scenarios such as nonstandard interactions and sterile neutrinos.

Before discussing the impact of the precision measurement of JUNO, we would like to point out that **T1** and **T2** are one-parameter patterns for the lepton mixing matrix, depending only on

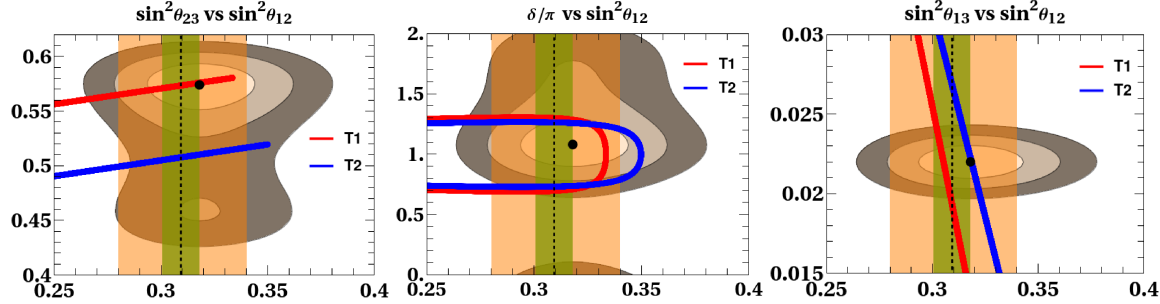


FIG. 2. The dashed black line gives to the best fit value of $\sin^2 \theta_{12}$ from JUNO with the corresponding 1σ , 3σ ranges shown in green and orange, respectively. The allowed 3σ C.L. global-fit parameters are shown in dark gray, with the 1σ , 2σ regions also displayed and the global best-fit marked (black dot). JUNO’s potential to test the **T1/T2** bi-large schemes is seen by comparing the red/blue regions with JUNO and global-fit results. See text for details.

the parameter ϕ , which is adjusted to reproduce all three mixing angles and the Dirac CP phase δ . Consequently, the mixing angles and δ are strongly correlated. For a detailed discussion, see Ref. [29]. The allowed range of ϕ is obtained by requiring all mixing angles and the Dirac phase δ to lie within their current 3σ experimental ranges [4]. By contrast, **T3** and **T4** depend on two parameters, ψ and ϕ . The allowed parameter regions for ψ and ϕ can be determined by fitting the current neutrino oscillation data, as discussed in Ref. [29]. In particular, the value of ψ is restricted to a narrow band around $\psi = 3$. In what follows we present the results of our numerical analysis for the various bi-large mixing schemes. Note that to obtain these we employ the exact formulae, rather than the leading-order approximations introduced in section II.

In the three panels of Fig. 2, we show our results for the **T1** and **T2** mixing patterns in the $(\sin^2 \theta_{12} - \sin^2 \theta_{23})$, $(\sin^2 \theta_{12} - \delta)$, and $(\sin^2 \theta_{12} - \sin^2 \theta_{13})$ parameter spaces, respectively. In each panel, the **T1** predictions are shown in the red regions, while **T2** predictions are indicated in blue. The oscillation parameters allowed at 3σ confidence level (C.L.) from the global-fit in [4] are shown in dark gray, with the corresponding 1σ and 2σ regions also displayed. The global best-fit value is marked by the black dot. The JUNO best-fit value is indicated by the dotted black line, and its associated 1σ and 3σ intervals are represented by the green and orange bands, respectively. The comparison of the blue and red regions with JUNO and global-fit results indicates the capability of JUNO to test the **T1** and **T2** bi-large mixing proposals.

The first remarkable result is seen from the first panel, namely that the **T1** pattern is compatible only with the higher atmospheric octant ($\sin^2 \theta_{23} > 0.5$), thereby excluding maximal atmospheric mixing ($\sin^2 \theta_{23} = 0.5$). Including the JUNO result further tightens the prediction to a narrow range around $\sin^2 \theta_{23} \simeq 0.57$. In contrast, as seen from the figure, we find that the **T2** pattern prefers nearly maximal mixing, $\sin^2 \theta_{23} \approx 0.5$ at 3σ .

The middle panel shows a very stringent restriction on the allowed Dirac CP phase δ . Imposing the latest JUNO constraint on $\sin^2 \theta_{12}$ splits the bi-large CP prediction into two branches, yielding

$\delta \approx 0.7\pi$ and 1.3π for the **T1** pattern at 1σ . This outcome disfavors both maximal CP violation ($\delta = \pm\pi/2$) as well as CP conservation ($\delta = \pi$) at 1σ . However the latter remains allowed at 3σ , as indicated by the red branch falling within the JUNO band (orange). In contrast, we note that the **T2** mixing pattern excludes CP conservation even at 3σ , since in this region of δ the blue branch lies outside the orange band.

Concerning the solar mixing parameter, from the first two panels, one sees that the **T1** pattern yields $\sin^2 \theta_{12} \sim (0.27 - 0.33)$, consistent with the global oscillation fit at 3σ . However, since θ_{13} is the most precisely measured mixing angle, the $(\sin^2 \theta_{12} \text{ vs. } \sin^2 \theta_{13})$ plane (third panel) gives a sharper restriction on the allowed region, yielding $\sin^2 \theta_{12} \sim (0.30 - 0.31)$. Likewise, the **T2** pattern limits $\sin^2 \theta_{12}$ to $\sim (0.315 - 0.325)$, as shown by the blue curve in the third panel.

The predictions for the **T3** and **T4** patterns are shown in Fig. 3. From the first panel, we see that the **T3** pattern is only marginally compatible with the global-fit range of $\sin^2 \theta_{23}$ at the 3σ level, and it predicts exclusively the lower octant (i.e., $\sin^2 \theta_{23} < 0.5$). In contrast, the **T4** pattern predicts an atmospheric mixing angle that is close to maximal.

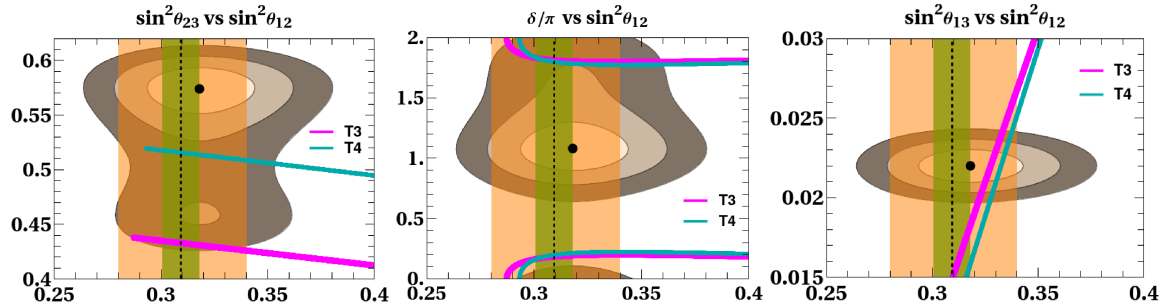


FIG. 3. Same as Fig. 2, but for type **T3** (magenta color) and **T4** (cyan color).

The middle panel shows that both the **T3** and **T4** patterns are excluded at the 2σ confidence level. However, at 3σ , one of the branches remains consistent with the global-fit. When the latest 1σ range from JUNO is included, the allowed region constrains the CP phase to lie near 1.8π , thereby excluding CP conservation. At the 3σ level, however, compatibility with CP conservation (i.e., $\delta = 2\pi$) is recovered. From the third panel, we see that while both patterns remain compatible with the global-fit to oscillation data at the 1σ level, they become excluded when the JUNO 1σ constraint is applied. However, at the 3σ level, the JUNO measurement is still compatible with both models. *Overall, the **T3** pattern is expected to be decisively tested—and potentially ruled out—by future precision measurements of $\sin^2 \theta_{23}$ and δ .*

V. NEUTRINOLESS DOUBLE BETA DECAY AFTER JUNO'S PRECISION MEASUREMENT

We now turn to the predictions for neutrinoless double beta ($0\nu\beta\beta$) decay within this framework. These involve also the Majorana phases, inaccessible to oscillation experiments, though the latter leave an imprint on the allowed values of the corresponding decay amplitude, determined by an effective Majorana mass parameter $\langle m_{\beta\beta} \rangle$. In the two panels of Fig. 4 we present $\langle m_{\beta\beta} \rangle$ as a function of the lightest neutrino mass m_1 for normal neutrino mass ordering, with the left panel corresponding to a generic scheme, while the right panel describes the $0\nu\beta\beta$ predictions for the **T1** bi-large mixing pattern in red and compares them with JUNO restrictions. The left panel of Fig. 4 shows how the region allowed by global the global oscillation fit (light purple) gets reduced by by using the current JUNO results (dark purple).

The right panel demonstrates that the bi-large pattern **T1** (red color region) fills a smaller region than allowed by the JUNO data. This is evident from the third panel of Fig. 2 that, when $\sin^2 \theta_{13}$ is taken within the 3σ range, the allowed values of θ_{12} for the **T1** pattern are more constrained than the JUNO results at the 3σ C.L. As the bi-large patterns do not predict mass-squared differences nor Majorana phases, all patterns **T1**, **T2**, **T3**, and **T4** have similar neutrinoless double beta decay predictions. Thus here we focus our discussion on the **T1** case only.

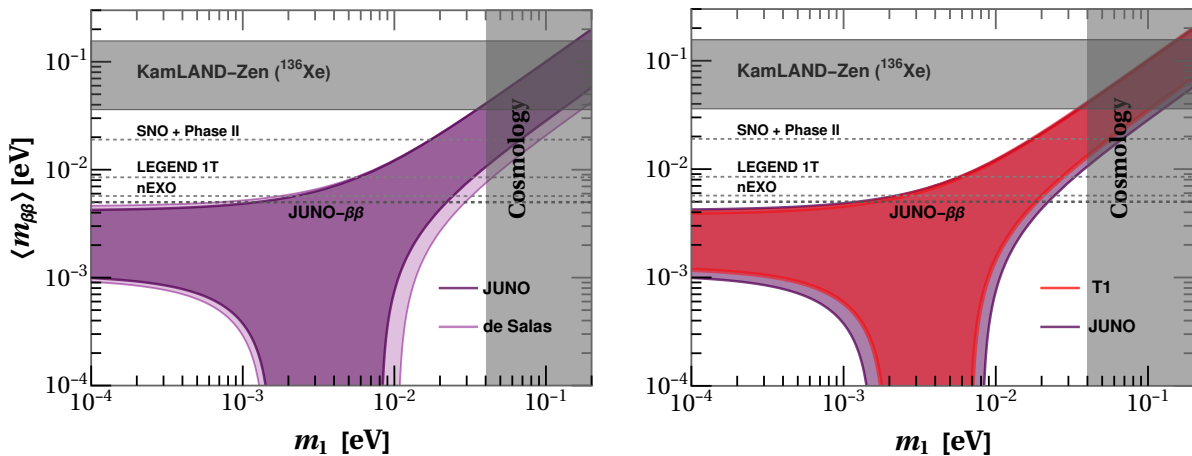


FIG. 4. Effective Majorana neutrino mass parameter $\langle m_{\beta\beta} \rangle$ as a function of the lightest active neutrino mass m_1 for normal ordering. The left panel compares the allowed $\langle m_{\beta\beta} \rangle$ region for a generic scheme before and after JUNO's results, shown in light and dark purple, respectively. The right panel compares the **T1** bi-large pattern (in red) with the JUNO results (dark purple). The current KamLAND-Zen limit and the projected sensitivities including JUNO are also indicated. The limit on m_1 from cosmology is shown in vertical gray band; see text for details.

All in all, one sees that there is a slight reduction in the allowed neutrinoless double beta decay region, stemming from JUNO's more precise measurements of θ_{12} and Δm_{21}^2 . As a visual guide we also show current experimental limits from KamLAND-Zen (36–156 meV) [48] as a horizontal gray

band and the projected sensitivities of next-generation experiments targeting $\langle m_{\beta\beta} \rangle \sim \mathcal{O}(10 \text{ meV})$ at 90% C.L.. These include JUNO- $\beta\beta$ (5 – 12 meV) [49], KamLAND2-Zen (< 20 meV) [50], LEGEND 1000 (8.5 – 19.4 meV) [51], nEXO (5.7 – 17.7 meV) [52], and SNO+ Phase II (19 – 46 meV) [53]. These experiments are expected to significantly improve the exploration of the allowed value of $\langle m_{\beta\beta} \rangle$, although a substantial portion of the normal-ordering region will remain beyond their reach. Their expected sensitivities are shown in both panels of the figure, which also displays the neutrino mass constraint from cosmological observations by Planck [54] as a gray vertical band.

VI. SUMMARY

We have described four bi-large patterns for the lepton mixing matrix. We examined the compatibility of these four mixing patterns by confronting their predictions with current oscillation data as well as the latest JUNO measurement. First we investigated their viability with global oscillation fits before JUNO, Fig. 1. By combining with the new JUNO constraint on $\sin^2 \theta_{12}$ the bi-large mixing predictions become cornered by stringent restrictions on the allowed parameter space, see Figs. 2 and 3. For the **T1** pattern in particular, several distinctive features emerge: it is incompatible with maximal CP violation, it rules out the possibility of CP conservation, and it forbids maximal atmospheric mixing. These characteristics make its predictions sharply distinctive. On the other hand, the **T2** pattern predicts nearly maximal $\sin^2 \theta_{23}$ and, concerning the CP phase, it exhibits predictive behavior similar to that of the **T1** pattern. Note that **T1** and **T2** are one-parameter schemes, characterized by a single parameter ϕ that determines all leptonic mixing angles and the Dirac CP phase δ . In contrast, the patterns **T3** and **T4** depend on two parameters, ψ and ϕ . However these patterns are severely cornered by the already existing data and are expected to be decisively tested and potentially excluded by future precision measurements of $\sin^2 \theta_{23}$ and δ . We have also discussed the implications of JUNO’s findings for neutrinoless double beta decay, Fig. 4.

ACKNOWLEDGMENTS

This work is funded by Spanish grants PID2023-147306NB-I00 and Severo Ochoa Excellence grant CEX2023-001292-S (AEI/10.13039/501100011033) and by Prometeo CIPROM/2021/054 of Generalitat Valenciana. GJD is supported by the National Natural Science Foundation of China under Grant No 12375104 and Guizhou Provincial Major Scientific and Technological Program XKBF (2025)010.

[1] **JUNO** Collaboration, A. Abusleme *et al.*, “First measurement of reactor neutrino oscillations at JUNO,” [arXiv:2511.14593 \[hep-ex\]](https://arxiv.org/abs/2511.14593).

[2] **SNO+** Collaboration, M. Abreu *et al.*, “Measurement of reactor antineutrino oscillations with 1.46 ktonne-years of data at SNO+,” [arXiv:2511.11856 \[hep-ex\]](https://arxiv.org/abs/2511.11856).

[3] **Particle Data Group and 2025 update** Collaboration, S. Navas *et al.*, “Review of particle physics,” *Phys. Rev. D* **110** no. 3, (2024) 030001.

[4] P. F. de Salas, D. V. Forero, S. Gariazzo, P. Martínez-Miravé, O. Mena, C. A. Ternes, M. Tórtola, and J. W. F. Valle, “2020 global reassessment of the neutrino oscillation picture,” *JHEP* **02** (2021) 071, [arXiv:2006.11237 \[hep-ph\]](https://arxiv.org/abs/2006.11237).

[5] P. F. De Salas *et al.*, “Chi2 profiles from Valencia neutrino global fit,” 2021. <https://doi.org/10.5281/zenodo.4726908>.

[6] I. Esteban, M. C. Gonzalez-Garcia, M. Maltoni, I. Martinez-Soler, J. P. Pinheiro, and T. Schwetz, “NuFit-6.0: updated global analysis of three-flavor neutrino oscillations,” *JHEP* **12** (2024) 216, [arXiv:2410.05380 \[hep-ph\]](https://arxiv.org/abs/2410.05380).

[7] F. Capozzi, W. Giarè, E. Lisi, A. Marrone, A. Melchiorri, and A. Palazzo, “Neutrino masses and mixing: Entering the era of subpercent precision,” *Phys. Rev. D* **111** no. 9, (2025) 093006, [arXiv:2503.07752 \[hep-ph\]](https://arxiv.org/abs/2503.07752).

[8] F. Capozzi, E. Lisi, F. Marcone, A. Marrone, and A. Palazzo, “Updated bounds on the (1,2) neutrino oscillation parameters after first JUNO results,” [arXiv:2511.21650 \[hep-ph\]](https://arxiv.org/abs/2511.21650).

[9] S. F. King, “Unified Models of Neutrinos, Flavour and CP Violation,” *Prog. Part. Nucl. Phys.* **94** (2017) 217–256, [arXiv:1701.04413 \[hep-ph\]](https://arxiv.org/abs/1701.04413).

[10] F. Feruglio and A. Romanino, “Lepton flavor symmetries,” *Rev. Mod. Phys.* **93** no. 1, (2021) 015007, [arXiv:1912.06028 \[hep-ph\]](https://arxiv.org/abs/1912.06028).

[11] Z.-z. Xing, “Flavor structures of charged fermions and massive neutrinos,” *Phys. Rept.* **854** (2020) 1–147, [arXiv:1909.09610 \[hep-ph\]](https://arxiv.org/abs/1909.09610).

[12] Y. Almumin, M.-C. Chen, M. Cheng, V. Knapp-Perez, Y. Li, A. Mondol, S. Ramos-Sanchez, M. Ratz, and S. Shukla, “Neutrino Flavor Model Building and the Origins of Flavor and CP Violation,” *Universe* **9** no. 12, (2023) 512, [arXiv:2204.08668 \[hep-ph\]](https://arxiv.org/abs/2204.08668).

[13] G. Chauhan, P. S. B. Dev, I. Dubovyk, B. Dziewit, W. Flieger, K. Grzanka, J. Gluza, B. Karmakar, and S. Zieba, “Phenomenology of lepton masses and mixing with discrete flavor symmetries,” *Prog. Part. Nucl. Phys.* **138** (2024) 104126, [arXiv:2310.20681 \[hep-ph\]](https://arxiv.org/abs/2310.20681).

[14] G.-J. Ding and S. F. King, “Neutrino mass and mixing with modular symmetry,” *Rept. Prog. Phys.* **87** no. 8, (2024) 084201, [arXiv:2311.09282 \[hep-ph\]](https://arxiv.org/abs/2311.09282).

[15] G.-J. Ding and J. W. F. Valle, “The symmetry approach to quark and lepton masses and mixing,” *Phys. Rept.* **1109** (2025) 1–105, [arXiv:2402.16963 \[hep-ph\]](https://arxiv.org/abs/2402.16963).

[16] W. Chao, “Quantum field theory approach to neutrino oscillations in dark matter and implications at JUNO,” [arXiv:2511.15494 \[hep-ph\]](https://arxiv.org/abs/2511.15494).

- [17] Y.-F. Li, A. Wang, Y. Xu, and J.-y. Zhu, “Terrestrial Matter Effects on Reactor Antineutrino Oscillations: Constant vs. Fluctuated Density Profiles,” [arXiv:2511.15702 \[hep-ph\]](https://arxiv.org/abs/2511.15702).
- [18] D. Zhang, “Trimaximal Mixing Patterns Meet the First JUNO Result,” [arXiv:2511.15654 \[hep-ph\]](https://arxiv.org/abs/2511.15654).
- [19] J. Huang and S. Zhou, “Probing unitarity violation of lepton flavor mixing matrix with reactor antineutrinos at JUNO and TAO,” [arXiv:2511.15525 \[hep-ph\]](https://arxiv.org/abs/2511.15525).
- [20] S.-F. Ge, C.-F. Kong, M. Lindner, and J. P. Pinheiro, “Neutrinoless Double Beta Decay in Light of JUNO First Data,” [arXiv:2511.15391 \[hep-ph\]](https://arxiv.org/abs/2511.15391).
- [21] Z.-z. Xing, “Divergence in tracing the flavors of astrophysical neutrinos: can JUNO help IceCube?,” [arXiv:2511.15127 \[hep-ph\]](https://arxiv.org/abs/2511.15127).
- [22] Z.-Q. Chen, G.-X. Fang, and Y.-L. Zhou, “Probing quark-lepton correlation in GUTs with high-precision neutrino measurements,” [arXiv:2511.16196 \[hep-ph\]](https://arxiv.org/abs/2511.16196).
- [23] X.-G. He, “Modified Tri-bimaximal neutrino mixing confront with JUNO θ_{12} measurement,” [arXiv:2511.15978 \[hep-ph\]](https://arxiv.org/abs/2511.15978).
- [24] W.-H. Jiang, R. Ouyang, and Y.-L. Zhou, “Modular TM₁ mixing in light of precision measurement in JUNO,” [arXiv:2511.16348 \[hep-ph\]](https://arxiv.org/abs/2511.16348).
- [25] S. M. Boucenna, S. Morisi, M. Tortola, and J. W. F. Valle, “Bi-large neutrino mixing and the Cabibbo angle,” *Phys. Rev. D* **86** (2012) 051301, [arXiv:1206.2555 \[hep-ph\]](https://arxiv.org/abs/1206.2555).
- [26] G.-J. Ding, S. Morisi, and J. W. F. Valle, “Bilarge neutrino mixing and Abelian flavor symmetry,” *Phys. Rev. D* **87** no. 5, (2013) 053013, [arXiv:1211.6506 \[hep-ph\]](https://arxiv.org/abs/1211.6506).
- [27] S. Roy, S. Morisi, N. N. Singh, and J. W. F. Valle, “The Cabibbo angle as a universal seed for quark and lepton mixings,” *Phys. Lett. B* **748** (2015) 1–4, [arXiv:1410.3658 \[hep-ph\]](https://arxiv.org/abs/1410.3658).
- [28] P. Chen, G.-J. Ding, R. Srivastava, and J. W. F. Valle, “Predicting neutrino oscillations with “bi-large” lepton mixing matrices,” *Phys. Lett. B* **792** (2019) 461–464, [arXiv:1902.08962 \[hep-ph\]](https://arxiv.org/abs/1902.08962).
- [29] G.-J. Ding, N. Nath, R. Srivastava, and J. W. F. Valle, “Status and prospects of ‘bi-large’ leptonic mixing,” *Phys. Lett. B* **796** (2019) 162–167, [arXiv:1904.05632 \[hep-ph\]](https://arxiv.org/abs/1904.05632).
- [30] **Daya Bay** Collaboration, F. P. An *et al.*, “Observation of electron-antineutrino disappearance at Daya Bay,” *Phys. Rev. Lett.* **108** (2012) 171803, [arXiv:1203.1669 \[hep-ex\]](https://arxiv.org/abs/1203.1669).
- [31] **Daya Bay** Collaboration, F. P. An *et al.*, “Measurement of electron antineutrino oscillation based on 1230 days of operation of the Daya Bay experiment,” *Phys. Rev. D* **95** no. 7, (2017) 072006, [arXiv:1610.04802 \[hep-ex\]](https://arxiv.org/abs/1610.04802).
- [32] **T2K** Collaboration, K. Abe *et al.*, “Combined Analysis of Neutrino and Antineutrino Oscillations at T2K,” *Phys. Rev. Lett.* **118** no. 15, (2017) 151801, [arXiv:1701.00432 \[hep-ex\]](https://arxiv.org/abs/1701.00432).
- [33] H. Minakata and A. Y. Smirnov, “Neutrino mixing and quark-lepton complementarity,” *Phys. Rev. D* **70** (2004) 073009, [arXiv:hep-ph/0405088](https://arxiv.org/abs/hep-ph/0405088).
- [34] C. H. Albright, A. Dueck, and W. Rodejohann, “Possible Alternatives to Tri-bimaximal Mixing,” *Eur. Phys. J. C* **70** (2010) 1099–1110, [arXiv:1004.2798 \[hep-ph\]](https://arxiv.org/abs/1004.2798).
- [35] P. Chen, G.-J. Ding, F. Gonzalez-Canales, and J. W. F. Valle, “Generalized $\mu - \tau$ reflection symmetry and leptonic CP violation,” *Phys. Lett. B* **753** (2016) 644–652, [arXiv:1512.01551 \[hep-ph\]](https://arxiv.org/abs/1512.01551).
- [36] P. Pasquini, S. C. Chuliá, and J. W. F. Valle, “Neutrino oscillations from warped flavor symmetry: predictions for long baseline experiments T2K, NOvA and DUNE,” *Phys. Rev. D* **95** no. 9, (2017) 095030, [arXiv:1610.05962 \[hep-ph\]](https://arxiv.org/abs/1610.05962).

[37] P. Chen, S. Centelles Chuliá, G.-J. Ding, R. Srivastava, and J. W. F. Valle, “Neutrino Predictions from Generalized CP Symmetries of Charged Leptons,” *JHEP* **07** (2018) 077, [arXiv:1802.04275 \[hep-ph\]](https://arxiv.org/abs/1802.04275).

[38] P. F. Harrison, D. H. Perkins, and W. G. Scott, “Tri-bimaximal mixing and the neutrino oscillation data,” *Phys. Lett. B* **530** (2002) 167, [arXiv:hep-ph/0202074](https://arxiv.org/abs/hep-ph/0202074).

[39] M. H. Rahat, P. Ramond, and B. Xu, “Asymmetric tribimaximal texture,” *Phys. Rev. D* **98** no. 5, (2018) 055030, [arXiv:1805.10684 \[hep-ph\]](https://arxiv.org/abs/1805.10684).

[40] P. Chen, S. Centelles Chuliá, G.-J. Ding, R. Srivastava, and J. W. F. Valle, “Realistic tribimaximal neutrino mixing,” *Phys. Rev. D* **98** no. 5, (2018) 055019, [arXiv:1806.03367 \[hep-ph\]](https://arxiv.org/abs/1806.03367).

[41] P. Chen, S. Centelles Chuliá, G.-J. Ding, R. Srivastava, and J. W. F. Valle, “CP symmetries as guiding posts: revamping tri-bi-maximal mixing. Part I,” *JHEP* **03** (2019) 036, [arXiv:1812.04663 \[hep-ph\]](https://arxiv.org/abs/1812.04663).

[42] S. S. Chatterjee, M. Masud, P. Pasquini, and J. W. F. Valle, “Cornering the revamped BMV model with neutrino oscillation data,” *Phys. Lett. B* **774** (2017) 179–182, [arXiv:1708.03290 \[hep-ph\]](https://arxiv.org/abs/1708.03290).

[43] R. Srivastava, C. A. Ternes, M. Tórtola, and J. W. F. Valle, “Testing a lepton quarticity flavor theory of neutrino oscillations with the DUNE experiment,” *Phys. Lett. B* **778** (2018) 459–463, [arXiv:1711.10318 \[hep-ph\]](https://arxiv.org/abs/1711.10318).

[44] R. Srivastava, C. A. Ternes, M. Tórtola, and J. W. F. Valle, “Zooming in on neutrino oscillations with DUNE,” *Phys. Rev. D* **97** no. 9, (2018) 095025, [arXiv:1803.10247 \[hep-ph\]](https://arxiv.org/abs/1803.10247).

[45] K. Chakraborty, K. N. Deepthi, S. Goswami, A. S. Joshipura, and N. Nath, “Exploring partial μ - τ reflection symmetry at DUNE and Hyper-Kamiokande,” *Phys. Rev. D* **98** no. 7, (2018) 075031, [arXiv:1804.02022 \[hep-ph\]](https://arxiv.org/abs/1804.02022).

[46] N. Nath, “Consequences of μ - τ Reflection Symmetry at DUNE,” *Phys. Rev. D* **98** no. 7, (2018) 075015, [arXiv:1805.05823 \[hep-ph\]](https://arxiv.org/abs/1805.05823).

[47] N. Nath, R. Srivastava, and J. W. F. Valle, “Testing generalized CP symmetries with precision studies at DUNE,” *Phys. Rev. D* **99** no. 7, (2019) 075005, [arXiv:1811.07040 \[hep-ph\]](https://arxiv.org/abs/1811.07040).

[48] KamLAND-Zen Collaboration, S. Abe *et al.*, “Search for the Majorana Nature of Neutrinos in the Inverted Mass Ordering Region with KamLAND-Zen,” *Phys. Rev. Lett.* **130** no. 5, (2023) 051801, [arXiv:2203.02139 \[hep-ex\]](https://arxiv.org/abs/2203.02139).

[49] J. Zhao, L.-J. Wen, Y.-F. Wang, and J. Cao, “Physics potential of searching for $0\nu\beta\beta$ decays in JUNO,” *Chin. Phys. C* **41** no. 5, (2017) 053001, [arXiv:1610.07143 \[hep-ex\]](https://arxiv.org/abs/1610.07143).

[50] R. Nakamura, H. Sambonsugi, K. Shiraishi, and Y. Wada, “Research and development toward KamLAND2-Zen,” *J. Phys. Conf. Ser.* **1468** no. 1, (2020) 012256.

[51] LEGEND Collaboration, N. Abgrall *et al.*, “The Large Enriched Germanium Experiment for Neutrinoless $\beta\beta$ Decay: LEGEND-1000 Preconceptual Design Report,” [arXiv:2107.11462 \[physics.ins-det\]](https://arxiv.org/abs/2107.11462).

[52] nEXO Collaboration, J. B. Albert *et al.*, “Sensitivity and Discovery Potential of nEXO to Neutrinoless Double Beta Decay,” *Phys. Rev. C* **97** no. 6, (2018) 065503, [arXiv:1710.05075 \[nucl-ex\]](https://arxiv.org/abs/1710.05075).

[53] SNO+ Collaboration, S. Andringa *et al.*, “Current Status and Future Prospects of the SNO+ Experiment,” *Adv. High Energy Phys.* **2016** (2016) 6194250, [arXiv:1508.05759 \[physics.ins-det\]](https://arxiv.org/abs/1508.05759).

[54] Planck Collaboration, N. Aghanim *et al.*, “Planck 2018 results. VI. Cosmological parameters,” *Astron. Astrophys.* **641** (2020) A6, [arXiv:1807.06209 \[astro-ph.CO\]](https://arxiv.org/abs/1807.06209). [Erratum: *Astron. Astrophys.* 652, C4 (2021)].